

Picosecond sampling with fiber-illuminated ErAs:GaAs photoconductive switches in a strong magnetic field and a cryogenic environment

M. Griebel, J. H. Smet,^{a)} J. Kuhl, and K. von Klitzing

Max-Planck-Institut für Festkörperforschung, Heisenbergstraße 1, 70569 Stuttgart, Germany

D. C. Driscoll, C. Kadow, and A. C. Gossard

Materials Department, University of California–Santa Barbara, Santa Barbara, California 93106-5050

(Received 27 January 2003; accepted 7 March 2003)

A sampling setup for a cryogenic environment has been developed using fiber-illuminated photoconductive switches fabricated from a material composed of equidistant layers of self-assembled ErAs nanoislands in a GaAs matrix. The setup includes dispersion compensation of the fibers and exhibits a time resolution better than 2.2 ps, which is insensitive to temperature and applied magnetic field and limited only by the properties of the coplanar waveguide circuitry. In cryogenic photocurrent autocorrelation measurements on single switches, a resolution exceeding 850 fs could be achieved. © 2003 American Institute of Physics. [DOI: 10.1063/1.1573367]

The impetus for the experiments described here originates from the long term desire of performing ultrafast time-resolved transport measurements on mesoscopic devices.¹ This goal imposes stringent simultaneous requirements: (i) a resolution well below 10 ps to cover the characteristic transit times and frequency scales of such devices, (ii) compatibility with the ultracold environment of dilution fridges, required for device operation ($T \ll 1$ K), as well as (iii) the applicability of a high B field, which represents an invaluable parameter to influence *in situ* the density of states. These conditions preclude all-electronic means and the use of coaxial lines. We pursue an all-on-one-chip photoconductive (PC) sampling solution,^{2–4} in which both the generation of the high frequency signals as well as their detection and down-conversion to quasi-dc signals proceeds in close proximity to the device under test. Fiber optics in conjunction with a dispersion compensation scheme for the several meters long fibers, demanded by high- B low- T cryostats, yield a technical implementation that satisfies the earlier criteria. The mature techniques to produce and chirp subpicosecond optical pulses are combined with the virtues of single mode fibers to bring these pulses nearly undistorted into such cryostats while avoiding excessive thermal loading from for instance optical windows. The entire method also hinges on the availability of suitable photoconductors that on the one hand succeed in transducing efficiently incident optical pulses in electrical pulses of comparable width despite the low T and presence of high B fields and on the other hand are compatible enough to allow monolithic integration with those materials needed to fabricate mesoscopic components.

The photoconductor chosen for our studies is made up of equidistant layers of self-assembled ErAs islands, which act as fast carrier trapping sites, inside a GaAs-matrix (ErAs:GaAs).^{5–8} It is grown by molecular beam epitaxy on a semi-insulating GaAs (100) substrate. On top of a 100 nm GaAs buffer layer, a superlattice of 40 periods of 1.2 monolayers of ErAs and 40 nm of GaAs is deposited at 530 °C.

The typical island diameter ranges from 1 to 2 nm and the estimated density equals $7 \times 10^{12} \text{ cm}^{-2}$.^{5,6} This material possesses a number of intriguing advantages over for example the most widely used photoconductor for sampling methods, low-temperature-grown GaAs (LTG–GaAs).⁸ The lifetime of photogenerated carriers can be engineered in a straightforward fashion by changing the superlattice period, i.e., the distance between adjacent ErAs islands layers.^{5,8} The trap density and the dark resistance are independently tunable by varying the island size and their density through an adjustment of the growth temperature and the amount of ErAs deposited.⁵ ErAs:GaAs is thermally stable up to 700 °C and displays excellent surface morphology despite the incorporated islands.^{5,6} These are the prerequisites that should enable the integration with high-quality GaAs/AlGaAs heterostructures, because—in contrast to LTG–GaAs—the microstructure, carrier dynamics, and dark resistance are left unaffected during the subsequent deposition of these additional layers.

The PC sampling circuit [Fig. 1(a)] consists of (i) a single PC switch (PCS) to excite short electrical pulses on the coplanar waveguide (CPW), (ii) a twin PCS to detect these pulses after propagation along the 1.5-mm-long main CPW, and (iii) the four 2.7 mm long “parasitic” CPWs to bias or contact the PCSs.² This geometry lends itself to the integration of mesoscopic components.³ Here we restrict ourselves to the characterization of a straight CPW section as some device under test. The circuit is fabricated in a single photolithography step by lifting off 400 nm of Au and a 10 nm Ti adhesion layer. The CPWs possess a 20 μm wide center conductor, separated by 10 μm gaps from the ground planes to achieve a characteristic impedance of 44 Ω . The interdigitated PCSs are made up of five fingers, 2 μm apart and 2.5 μm wide. The pump switch has an area of $20 \times 20 \mu\text{m}^2$ and an estimated capacitance of 4.7 fF (RC time of 210 fs). Each of the probe switches covers an area of $15 \times 20 \mu\text{m}^2$ corresponding to 4.0 fF (180 fs). In this twin probe-switch configuration, the undesirable lossy and dispersive even waveguide mode can be distinguished from the odd mode as an imbalance between the top and bottom signals.^{2,3} Both the pump and probe PCSs were coupled to

^{a)}Electronic mail: j.smet@fkf.mpg.de

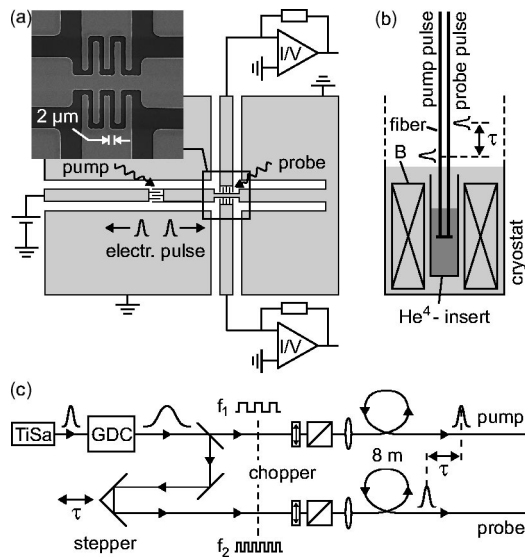


FIG. 1. (a) Schematic diagram of the coplanar waveguide circuit. The inset shows a scanning electron microscopy picture of the twin probe-switch. (b) Sketch of a fiber coupled sample in the ⁴He bath-cryostat. (c) Optical setup for the PC sampling experiments.

8 m long single mode fibers with a numerical aperture (NA) of 0.16 [Fig. 1(b)]. The fiber ends were cemented with an UV-curing transparent adhesive roughly 50 μm above the sample surface, resulting in an illuminated spot diameter of about 16 μm. Before curing, the fibers were aligned either by maximizing the dc photocurrent through the pump switch or by balancing the currents through both probe switches.

PC sampling was performed by splitting a 120 fs pulse train from a mode-locked titanium-sapphire laser operating at 800 nm with a repetition rate of 76 MHz. The beams were mechanically chopped at different frequencies and one of them was delayed with respect to the other with a retroreflector mounted onto a stepper motor driven translation stage. The pulse trains illuminated the pump and probe switches through the fibers [Fig. 1(c)]. The fiber dispersion was precompensated with the help of a grating-dispersion compensator. For 8 m long fibers, a full width at half maximum (FWHM) of 220 fs for 4 mW pulses at the fiber output (determined by second harmonic autocorrelation) could be achieved. Without compensation, pulse broadening is excessive and the pulse width is estimated at 8 ps.⁹ It may even be larger when considering self-phase modulation, likely to occur at the high peak powers. Both probe currents pass through low noise transimpedance amplifiers, whose signals were recorded as a function of the delay using sum-frequency lock-in detection.

Figure 2 shows the results at 295 and 4.2 K with and without a B field perpendicular to the sample surface. The main signal peak labeled *a* exhibits a FWHM of 2.2 ps irrespective of temperature and magnetic field strength. The B -field insensitivity is ascribed to the use of lifetime limited ErAs:GaAs PCSs and contrasts with the strong field dependent behavior in transit-time limited switches based on standard GaAs.¹⁰ The excellent signal-to-noise ratio at these low power levels promises the successful implementation of the experiment in cryostats, that offer temperatures in the 50 mK range but at the same time suffer from limited cooling power of a few hundred microwatts only. At room temperature, an

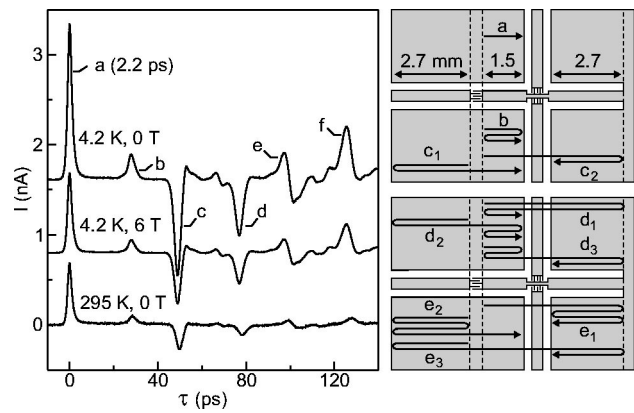


FIG. 2. Sampling measurements at 295 and 4.2 K with and without a magnetic field perpendicular to the sample surface. Curves are offset for clarity. The bias voltage of the pump switch is 10 V, the average incident light power on the pump and the probe switches is 175 μW. The right panel displays the waveguide dimensions and the various propagation paths of the electrical pulses on the CPW, which contribute to the reflection peaks labeled b–e. Peak *f* originates from combinations of paths *e* with *b*.

identical time resolution was found when employing free space optics. From photocurrent autocorrelation measurements, a lifetime of 450 fs was extracted for the 40 nm ErAs:GaAs digital composite used here.⁸ These observations in conjunction with simulations of the pulse generation, propagation and detection identify the capacitance of the PCSs and the dispersion on the 1.5 mm long CPW as the main limiting factors for the time resolution. The secondary peaks in Fig. 2 labeled b–f can be unambiguously attributed, based on their time of arrival at the probe switches, to reflections at interruptions and short circuited ends of the central conductor or at the various geometrical discontinuities where impedances do not perfectly match. Due to the symmetry of the circuit, multiple reflection paths of equal total length contribute to peaks c–f. The T dependence of the peak amplitudes is likely caused by a slight mechanical displacement of the fiber endface during cooling due to differences in the thermal expansion of the sample holder, the sample, the optical cement, and the fiber itself. This assertion is supported by the observation of nonsystematic behavior of the amplitude when comparing different cooling cycles. The field dependence of the peak amplitudes is traced back to the positive magnetoresistance of the ErAs:GaAs under illumination, as illustrated in Fig. 3(a). Whereas the overall negative magnetoresistance in the dark (also shown) has been successfully

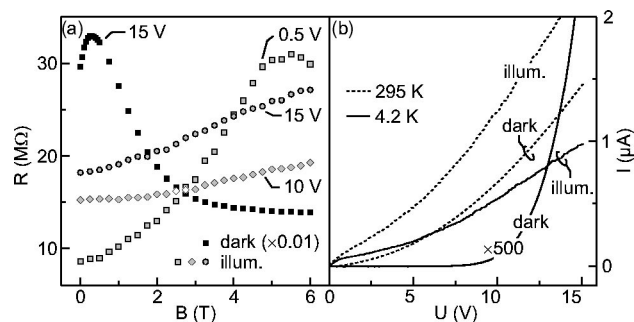


FIG. 3. (a) Magnetoresistance of the pump switch in the dark and under a 350 μW average illumination for different voltages at a temperature of 4.2 K. (b) Current-voltage characteristics of the pump switch under the same illumination conditions without magnetic field at 295 and 4.2 K.

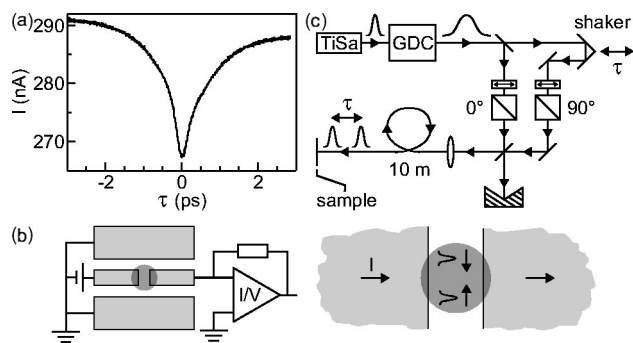


FIG. 4. (a) Photocurrent autocorrelation measurements on a sample coupled to an optical fiber of 10 m length at a temperature of 4.2 K. The asymmetry is ascribed to a slight misorientation of the polarization direction of the light with respect to the metallic edges of the CPW (see Ref. 8). The PCS was biased with a voltage of 2.25 V and illuminated with an average power of 2 mW per beam. (b) Sample geometry and (c) optical setup for the autocorrelation measurements.

accounted for by fluctuation-controlled hopping of bound magnetic polarons between ErAs islands,¹¹ the origin of the positive magnetoresistance under illumination as well as its voltage dependence have not been entirely resolved. Note that in this case conduction proceeds largely via photogenerated carriers in the GaAs matrix material itself. The orientation of Er-related moments may provide a field dependent scattering potential. Also the nonlinear properties of the non-alloyed contacts may play a role [Fig. 3(b)].

The intrinsic time resolution of our setup is subpicosecond, but is masked in pulse propagation experiments by the waveguide dispersion and switch capacitances. A photocurrent autocorrelation measurement is better suited to test the ultimate resolution, since neither of them affects its result. The temporal width of the correlation signal is determined mainly by the lifetime of the photogenerated mobile charges and the duration of the optical pulses.⁸ A 3 μm broad gap in the center conductor of a CPW made of 10 nm Ti and 200 nm Au forms a single PC switch [Fig. 4(b)]. It is illuminated in a collinear pump-probe arrangement [Fig. 4(c)] via 10 m of polarization maintaining panda-type fiber with a NA of 0.11. The illuminated spot size is 7 μm for a distance between PCS and fiber endface of roughly 30 μm . The pump and probe beams are carefully linearly cross polarized to avoid interference effects at their zero delay point. Starting from 120 fs input pulses, the fiber-dispersion compensation scheme for these polarization preserving fibers achieves a FWHM of 370 fs for 5.2 mW fiber-output pulses. The photocurrent flowing between the biased ends of the CPWs center conductor is detected with a transimpedance amplifier

and monitored with a sampling scope as a function of the delay between both pulse trains. The latter is varied periodically at a frequency of 16 Hz [Fig. 4(c)]. Averaging over some hundred delay cycles overcomes the intensity noise of the laser system. The autocorrelation measurements in Fig. 4(a) yield an upper limit for the electron lifetime of 850 fs. Within the experimental accuracy of ± 70 fs, this value coincides with the lifetime obtained with fiber coupled devices at room temperature. The discrepancy with the 450 fs found with free space optics is likely accounted for by the smaller illuminated spot size, i.e., tighter focusing, achieved with free space optics. Due to the finite spot size, the distributed character of the signal generation may no longer be ignored. The gap in the CPW acts as a minislotted line. Electrical transients generated at the spot extremities [as illustrated in Fig. 4(b)] propagate along this slotline and continue to contribute to the autocorrelation signal until they reach the other end of the spot. It artificially broadens the autocorrelation signal. We anticipate that with an optimization of the butt coupling, aimed at producing a smaller, well-centered spot size, the time resolution will approach the limit reached with free space optics. Already without it, the present setup offers bright prospects for ultrafast time-resolved transport investigations at low temperatures and high magnetic fields.

The authors acknowledge R. Wyss and R. Gerhardt for discussions. This research was supported by the DFG, JPL, and QUEST.

¹ *Mesoscopic Physics and Electronics*, edited by T. Ando, Y. Arakawa, K. Furuya, S. Komiyama, and H. Nakashima (Springer, Berlin, 1998).

² J. Lee, H. Lee, W. Kim, J. Lee, and J. Kim, *IEEE Microwave Guid. Wave Lett.* **9**, 265 (1999).

³ N. Zamdmer, Qing Hu, S. Verghese, and A. Förster, *Appl. Phys. Lett.* **74**, 1039 (1999).

⁴ S. Verghese, N. Zamdmer, Qing Hu, and A. Förster, *Appl. Phys. Lett.* **70**, 2644 (1997).

⁵ C. Kadow, S. B. Fleischer, J. B. Ibbetson, J. E. Bowers, A. C. Gossard, J. W. Dong, and C. J. Palmström, *Appl. Phys. Lett.* **75**, 3548 (1999).

⁶ C. Kadow, J. A. Johnson, K. Kolstad, J. P. Ibbetson, and A. C. Gossard, *J. Vac. Sci. Technol. B* **18**, 2197 (2000).

⁷ C. Kadow, A. W. Jackson, A. C. Gossard, S. Matsuura, and G. A. Blake, *Appl. Phys. Lett.* **76**, 3510 (2000).

⁸ M. Griebel, J. H. Smet, D. C. Driscoll, J. Kuhl, C. Alvarez Diez, N. Freytag, C. Kadow, A. C. Gossard, and K. von Klitzing, *Nat. Mater.* **2**, 122 (2003).

⁹ L. B. Jeunhomme, *Single-Mode Fiber Optics*, 2nd ed. (Marcel Dekker, New York, 1989), p. 128.

¹⁰ G. Ernst, R. J. Haug, M. Klingenstein, J. Kuhl, K. von Klitzing, and K. Eberl, *Appl. Phys. Lett.* **68**, 3752 (1996).

¹¹ D. R. Schmidt, A. G. Petukhov, M. Foygel, J. P. Ibbetson, and S. J. Allen, *Phys. Rev. Lett.* **82**, 823 (1999).